JOM, Vol. 71, No. 3, 2019
https://doi.org/10.1007/s11837-018-3210-8

SOLID FREEFORM FABRICATION

Effect of Process Parameters on Mechanical Properties of Wire and Arc Additive-Manufactured AlCu6Mn

YAZHOU ZHANG,[1] MING GAO,[1,2] and XIAOYAN ZENG[1]

1.—Wuhan National Laboratory for Optoelectronics (WNLO), Huazhong University of Science and Technology, Wuhan, Hubei 430074, People's Republic of China. 2.—e-mail: mgao@mail.hust.edu.cn

Wire and arc additive manufacturing (WAAM) is an additive manufacturing technique that can directly fabricate large three-dimensional parts. A variable-polarity cold metal transfer pulse arc was employed to melt metal wire onto a substrate. Tensile tests and microscopy were conducted to investigate the effects of the heat input on the mechanical properties and microstructure of the AlCu6Mn after WAAM deposition. The highest tensile strength of 295 MPa and tensile elongation of 18% were obtained with appropriate heat input. Also, the bottom region of the sample exhibited the best mechanical properties, followed by the middle and top region under the same parameters. This is mainly due to the increase of overburn defects and grain size in the top region with heat accumulation in the repeated thermal cycle.

INTRODUCTION

Wire and arc additive manufacturing (WAAM) is an additive manufacturing technique that can directly fabricate large three-dimensional (3D) parts from melted metal wire. It uses an electric arc as the heat source and metal wire as the feed material.[1–3] Recently, many researchers have indicated that arc sources offer many advantages over laser or electron beam power sources in terms of efficiency and economy.[4–8] Due to its higher deposition rate and material usage efficiency and low equipment costs, WAAM has attracted much interest for implementation in aerospace applications, e.g., for manufacture of large, meter-scale metallic parts.[9,10]

Large-size parts made from Al alloys, such as rocket propellant tanks, have been increasingly used in aerospace applications because of their high specific strength and good corrosion resistance. However, metallurgical defects can be formed easily in Al alloys. Use of a suitable electric arc is thus a critical success factor for WAAM of Al alloy parts.

Due to the anti-direction pulling function of the filler wire to assist with droplet detachment, the variable-polarity cold metal transfer (VP-CMT) process can significantly reduce the heat input. Compared with the common CMT process, the VP-CMT process using a variable-polarity arc provides effective oxide cleaning of the filler wire and previous deposition layer alternately. The VP-CMT mode should therefore represent an excellent process to weld or deposit Al alloys. Cong et al. found that the VP-CMT arc process eliminates porosity efficiently and confirmed that the key factors are the low heat input and negative-pole atomization.[11]

However, the effects of process parameters on the mechanical properties and microstructure of AlCu6Mn parts formed by WAAM in VP-CMT arc mode have rarely been researched to date. In the work presented herein, the effects of different process parameters on the tensile strength and elongation were carefully analyzed, and the relationships between the metallurgical defects and mechanical properties were researched.

EXPERIMENTAL PROCEDURES

Experiments were carried out using the experimental setup shown in Fig. 1, consisting of a Fanuc industrial robot to provide precise movement, a Fronius CMT-Advanced power source, and a VR7000 wire feeder. AlCu6Mn alloy wire with diameter of 1.2 mm was used as the feeding material. The chemical constituents of the AlCu6Mn alloy wire are presented in Table I. Al alloy (2A12) substrate with thickness of 20 mm and 99.99% argon were applied. Thin-wall components were

 (Published online October 31, 2018)

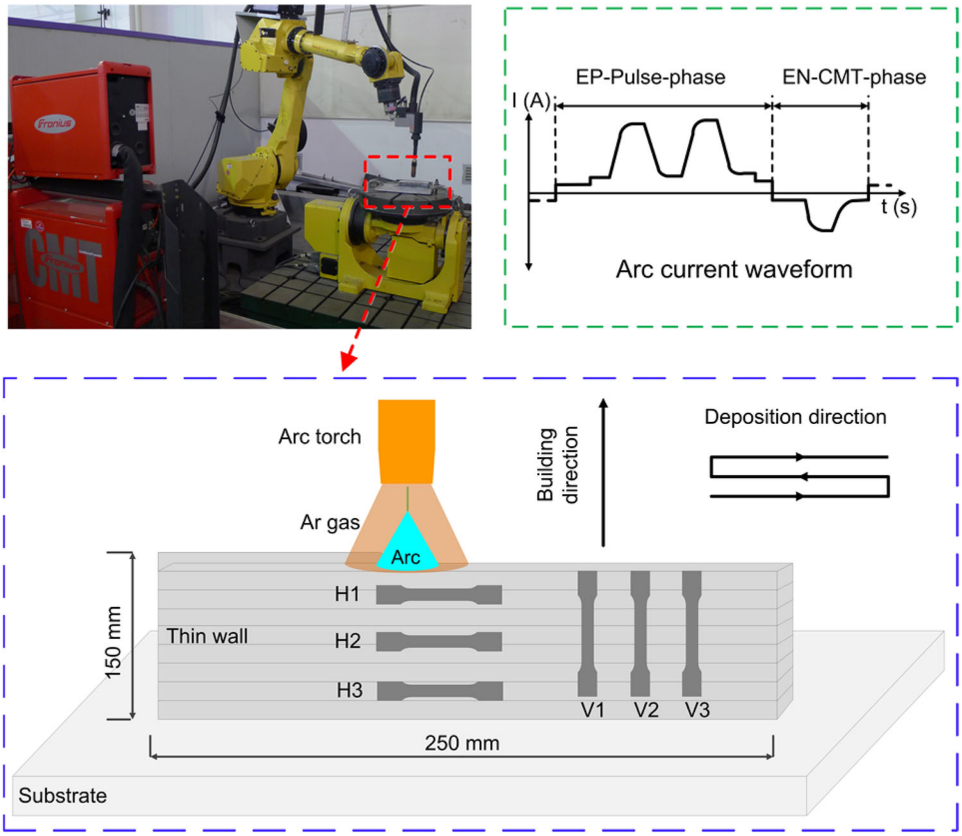

Fig. 1. Schematic diagram of the WAAM process.

Table I. Chemical constituents of AlCu6Mn alloy wire (wt.%)

Elements	Cu	Mn	Si	Mg	Fe	Zn	Ti	Al
Content	5.8–6.8	0.2–0.4	0.2	0.02	0.3	0.1	0.1–0.2	Bal.

produced in VP-CMT arc mode, which consists of an electrode positive (EP) pulse phase and an electrode negative (EN) CMT phase as shown in Fig. 1. To avoid overheating, the next layer was deposited after waiting for 60 s. As shown in Table II, L16 (4^5) orthogonal experiments were designed to study the effects of the arc current, the ratio of the EP to EN phase, the scanning speed, and the argon flow rate on the tensile strength and elongation. The ratio of the EP to EN phase represents the time ratio of the EP pulse phase to the electrode negative CMT phase overall the whole cycle of the VP-CMT arc mode.

Tensile samples V1 to V3 and H1 to H3 were cut along the vertical and horizontal direction of thin walls, respectively, using wire electrical discharge machining. Tensile testing was conducted following ASTM E8/E8M-15a standard. The dimensions of the samples are shown in Fig. 2. An anisotropy percentage was calculated for the tensile strength based on the tensile test results, calculated as

$$A = (S_h - S_v)/S_h \times 100\%, \quad (1)$$

where A represents the anisotropy percentage, and S_h and S_v are the average horizontal and vertical tensile strength, respectively.

Metallographic specimens were cut from cross-sections at different heights. After grinding and polishing, the specimens were etched using Keller's reagent for 50 s. A Nikon optical microscope (OM) was applied to observe the microstructure.

RESULTS AND DISCUSSION

Macromorphology

Figure 3 shows a typical thin-wall part and its cross section. Note that the surface of the thin wall is uniform and well formed. The use of a staggered deposition strategy improves the appearance of the deposit and fills the arc craters that are frequently caused at the arc starting and end points. Both side surfaces of the thin wall appear slightly serrated because of the layer-by-layer deposition mode. The effective width percentage of the cross section is as

Table II. Processing parameters of orthogonal experiments

Sample number	Arc current (A)	Ratio of EP to EN phase	Scanning speed (mm s^{-1})	Argon flow rate (L min^{-1})
#1	85	1.1	5	30
#2	85	1.0	6	25
#3	85	0.9	7	20
#4	85	0.8	8	15
#5	95	1.1	6	20
#6	95	1.0	5	15
#7	95	0.9	8	30
#8	95	0.8	7	25
#9	105	1.1	7	15
#10	105	1.0	8	20
#11	105	0.9	5	25
#12	105	0.8	6	30
#13	115	1.1	8	25
#14	115	1.0	7	30
#15	115	0.9	6	15
#16	115	0.8	5	20

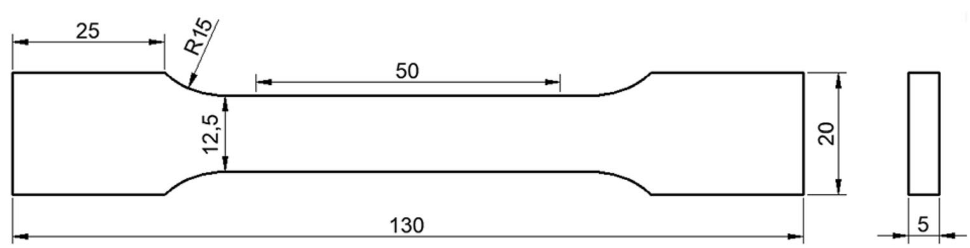

Fig. 2. Tensile test specimens used in the study.

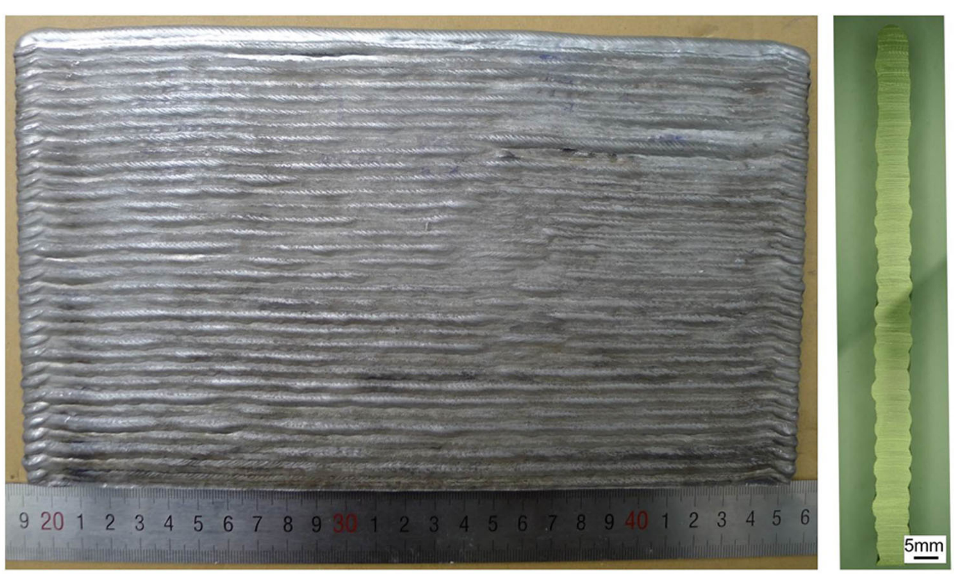

Fig. 3. Typical appearance and cross section of thin wall.

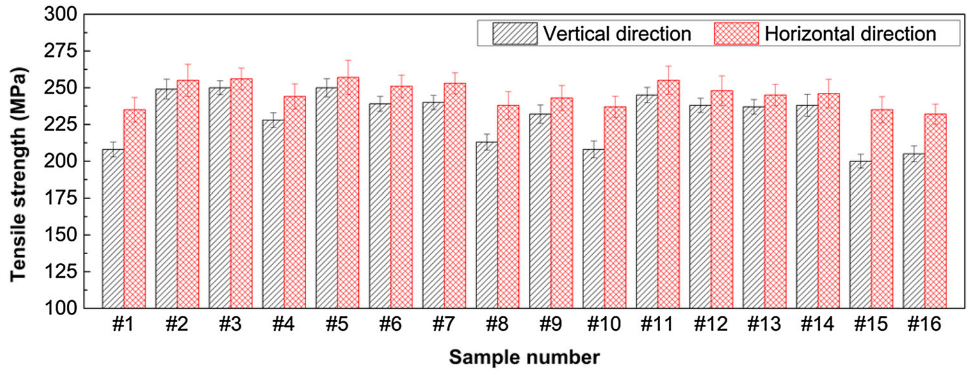

Fig. 4. Tensile strength of thin walls #1 to #16.

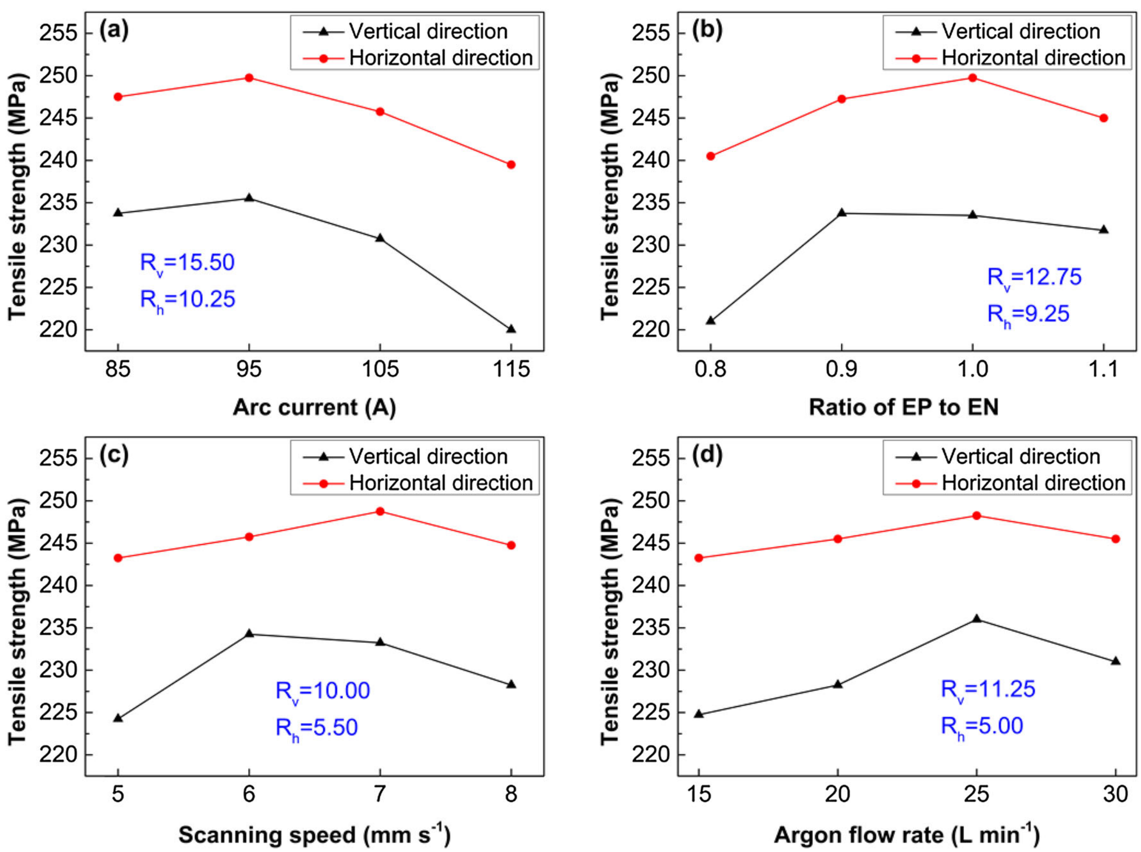

Fig. 5. Tensile strength as function of (a) arc current, (b) ratio of EP to EN phase, (c) scanning speed, and (d) argon flow rate.

high as 72%, which can effectively reduce mechanical process and production costs.

Mechanical Properties

Figure 4 shows the average tensile strength in the vertical and horizontal direction of thin walls #1 to #16 obtained using the process parameters given in Table II. Compared with all the vertical samples, all the horizontal samples exhibited higher tensile strength when using the same parameters. The anisotropy percentage ranged from 2.3% to 14.9%, but without showing any regularity.

As shown in Fig. 5, the effects of the four key process factors on the tensile strength were analyzed based on the results shown in Fig. 4. Note that the tensile strength first increased then decreased as the arc current was increased from 85 A to 115 A. The highest strength was achieved when using arc current of 95 A. These results also indicate that high quality in terms of properties and microstructure cannot be obtained when using a higher or

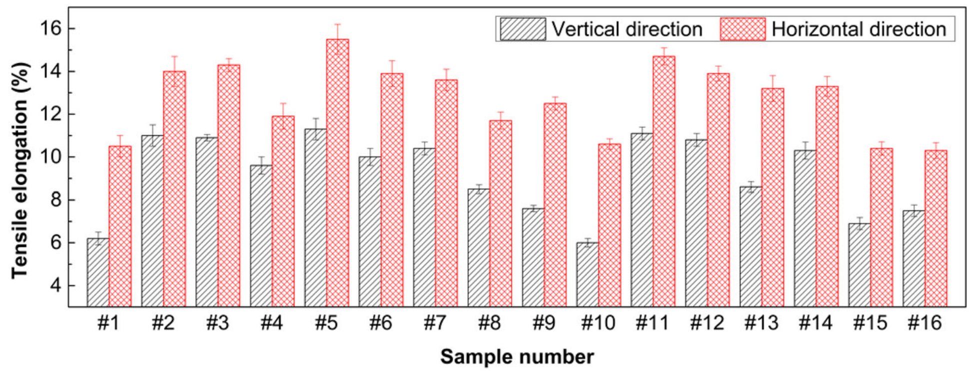

Fig. 6. Tensile elongation of thin walls #1 to #16.

lower arc current, which is a crucial factor for the heat input in the deposition process. In general, the smaller the ratio of the EP to EN phase, the better the cathode cleaning effect on the filler wire, but the lower the heat input and the worse the stability of the arc during the WAAM process. Even though pores can be decreased by negative-pole atomization, the tensile properties of thin walls are not the best when the ratio of the EP to EN phase was 0.8. The highest tensile strength in the vertical and horizontal direction was obtained when using a ratio of EP to EN phase of 0.9 and 1.0, respectively. With increase of the scanning speed, the tensile strength values first increased then decreased. There was a noticeable decline in the stability of the deposition and process when the scanning speed was increased from 7 mm/s to 8 mm/s. The argon flow rate primarily influences the shielding effect on the arc and molten pool. When it was changed from 15 L/min to 25 L/min, the tensile strength values in both directions gradually increased. However, the mechanical properties started to deteriorate observably at argon flow rates above 25 L/min, probably because an excessively high argon flow rate causes argon turbulence and results in air around the arc being included into the weld pool, which can significantly increase the amount of hydrogen pores in the deposited layers.

Comparing the ranges of the four factors shown in Fig. 5, the factors affected the tensile strength in the vertical direction in the order arc current, ratio of EP to EN phase, argon flow rate, and scanning speed. For the horizontal tensile strength, however, this order was arc current, ratio of EP to EN phase, scanning speed, and argon flow rate.

Figure 6 shows the average tensile elongation in the vertical and horizontal direction of thin walls #1 to #16. As found for the tensile strength, the elongation in the vertical direction was lower than that in the horizontal direction for the same parameter values. The effects of the factors on the tensile elongation was analyzed and is shown in Fig. 7, revealing a similar trend of influence to the effects on the tensile strength above. With increasing arc current, ratio of EP to EN phase, and scanning speed, the elongation also first increased then decreased, reaching a maximum at arc current, ratio of EP to EN phase, and scanning speed of 95 A, 0.9, and 6 mm/s, respectively. Besides, no regularity was observed in the effect of the argon flow rate on the elongation of the samples in the vertical direction. Based on the ranges of the factors, their effect on the elongation in the vertical direction was in the order arc current, ratio of EP to EN phase, scanning speed, and argon flow rate. For the elongation in horizontal direction, however, this order was arc current, ratio of EP to EN phase, argon flow rate, and scanning speed.

The analysis above shows that the WAAMed AlCu6Mn alloys exhibited greatly enhanced mechanical properties in the horizontal compared with the vertical direction. The arc current and the ratio of the EP to EN phase showed obvious effects on the tensile performance. The optimal parameters were obtained as arc current of 95 A, ratio of EP to EN phase of 0.9, scanning speed of 6 mm/s, and argon flow rate of 25 L/min, which can result in moderate thermal input and good arc stability during the WAAM process in the VP-CMT arc mode.

To verify the effectiveness of these optimal parameter values, a thin-wall component was fabricated using the optimal parameters; its mechanical properties were tested and are shown in Fig. 8. The average tensile strength and elongation in the vertical direction reached 253 MPa and 14.7%, respectively. Similarly, the horizontal samples exhibited excellent mechanical properties, with average tensile strength of 285 MPa and elongation of 17.2%. Even though the anisotropy percentage was 11.2%, the tensile properties of the thin wall obtained using the optimal parameter values exhibited far better performance compared with samples #1 to #16, especially in the horizontal direction. These results also strongly demonstrate the feasibility and effectiveness of the optimal parameter values, resulting in WAAMed AlCu6Mn alloys with acceptable mechanical properties.[12]

Notably, the mechanical properties of the vertical samples V1 to V3 are near to each other, while the tensile strength and elongation of sample H1 were

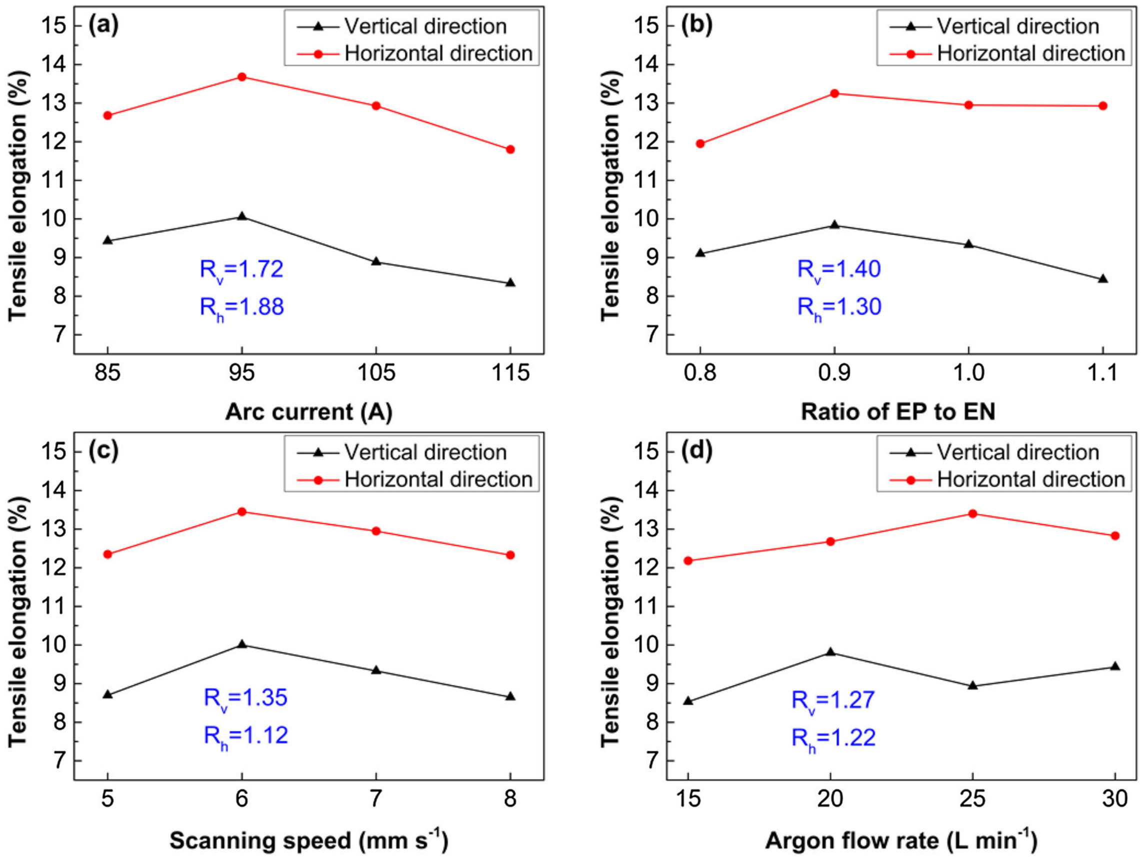

Fig. 7. Tensile elongation as function of (a) arc current, (b) ratio of EP to EN phase, (c) scanning speed, and (d) argon flow rate.

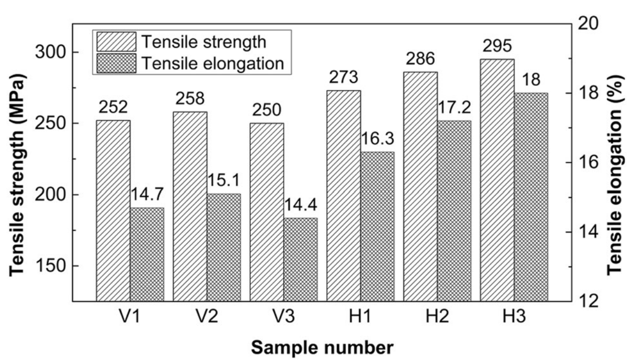

Fig. 8. Tensile properties of thin wall obtained with optimal parameter values.

about 7.5% and 9.4% lower than those of sample H3, respectively, which also applied to most of the thin walls #1 to #16 as well. To study this difference in tensile performance, etched cross sections cut from the top and bottom regions of a thin wall are shown in Fig. 9. Both regions exhibited some hydrogen pores and black overburn defects at the grain boundary. However, the overburn defects were more widespread and continuous in the top region. This is because the deposited material has to be heated many times by thermal cycles during the additive manufacturing process. As more layers are deposited, heat gradually accumulates in the thin wall, and thus more grain boundaries are remelted and overburnt. Besides, due to the overheating of the microstructure, grains in the top region are coarser than those in the bottom region. Both the overburn defects at the grain boundary and coarse grains can significantly deteriorate the mechanical properties. Therefore, the bottom region of the thin wall exhibited the best mechanical properties, followed by the middle and top region under the same parameters. More detailed and deep understanding of the relationship between metallurgical defects and the mechanical properties of WAAMed AlCu6Mn alloys will require further research.

CONCLUSION

AlCu6Mn alloy thin-wall components with uniform profile were fabricated by arc wire additive manufacturing using a VP-CMT arc power source. The effects of process parameters on mechanical properties were investigated. The following conclusions can be drawn:

1. WAAMed AlCu6Mn alloys show greatly enhanced mechanical properties in the horizontal compared with the vertical direction, while the anisotropy percentage varies without regularity.
2. Compared with the scanning speed and argon

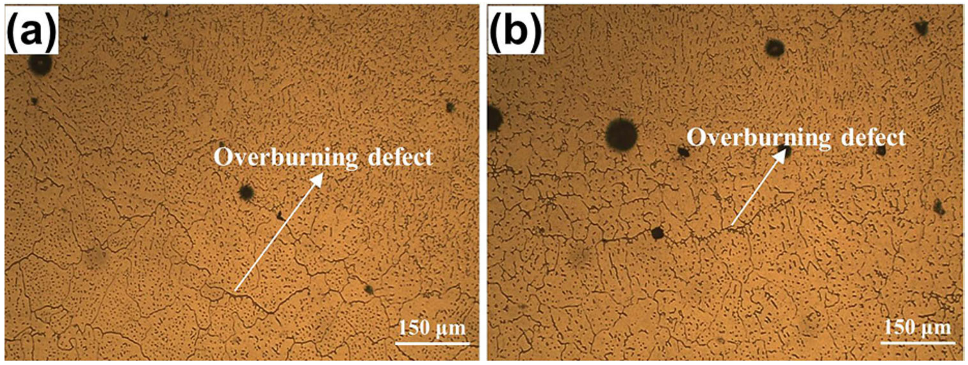

Fig. 9. Cross-sectional micrographs of (a) top region and (b) bottom region.

flow rate, the arc current and ratio of EP to EN phase showed more obvious effects on the tensile performance. The optimal parameters were obtained as arc current of 95 A, ratio of EP to EN phase of 0.9, scanning speed of 6 mm/s, and argon flow rate of 25 L/min.

3. A thin wall deposited using these optimal parameter values exhibited average tensile strength and elongation in the vertical direction of 253 MPa and 14.7%, respectively, while the average strength and elongation in the horizontal direction reached 285 MPa and 17.2%, respectively.
4. The mechanical properties in the top region of the thin wall were lower than those in the bottom region. This is mainly due to the increase of overburn defects and grain size in the top region with heat accumulation in the repeated thermal cycle during the WAAM process.

ACKNOWLEDGEMENTS

This research is financially supported by the National Natural Science Foundation of China (Grant Nos. 51775206 and 51429501). The authors would like to thank the Analytical and Testing Center of Huazhong University of Science and Technology.

REFERENCES

1. J. Gu, J. Ding, S.W. Williams, H. Gu, P. Ma, and Y. Zhai, *J. Mater. Process. Technol.* 230, 26 (2016).
2. J. Gu, J. Ding, S.W. Williams, H. Gu, J. Bai, Y. Zhai, and P. Ma, *Mater. Sci. Eng., A* 651, 18 (2016).
3. D. Ding, Z. Pan, D. Cuiuri, and H. Li, *Int. J. Adv. Manuf. Tech.* 81, 465 (2015).
4. W. Aiyiti, W. Zhao, and B. Lu, *Rapid Prototyping J.* 12, 165 (2006).
5. L. Liu, Z. Zhuang, F. Liu, and M. Zhu, *Int. J. Adv. Manuf. Tech.* 69, 2131 (2013).
6. F. Wang, S.W. Williams, P. Colegrove, and A. Antonysamy, *Metall. Mater. Trans. A* 44, 968 (2013).
7. J. Xiong and G. Zhang, *J. Mater. Process. Technol.* 214, 962 (2014).
8. D. Clark, M.R. Bache, and M.T. Whittaker, *J. Mater. Process. Technol.* 203, 439 (2008).
9. S.W. Williams, F. Martina, A.C. Addison, J. Ding, G. Pardal, and P. Colegrove, *Mater. Sci. Technol.* 32, 641 (2016).
10. Z. Pan, D. Ding, B. Wu, D. Cuiuri, H. Li, and J. Norrish, *Trans. Intell. Weld. Manuf.* 1, 3 (2018).
11. B. Cong, J. Ding, and S. Williams, *Int. J. Adv. Manuf. Tech.* 76, 1593 (2015).
12. ISO, *Wrought Aluminium and Aluminium Alloys. Sheets, Strips and Plates. Part 2: Mechanical Properties*. ISO 6361-2 (2014).